THE JOURNAL OF BIOLOGICAL CHEMISTRY Vol. 279, No. 7, Issue of February 13, pp. 5621–5629, 2004
Printed in U.S.A.

Role for ELOVL3 and Fatty Acid Chain Length in Development of Hair and Skin Function*

Received for publication, September 23, 2003, and in revised form, October 23, 2003
Published, JBC Papers in Press, October 27, 2003 DOI 10.1074/jbc.M310529200

Rolf Westerberg‡, Petr Tvrdik‡¶¶, Anne-Birgitte Undén§, Jan-Erik Månsson¶, Lars Norlén‖, Andreas Jakobsson‡, Walter H. Holleran, Peter M. Elias**, Abolfazl Asadi‡, Per Flodby¶¶, Rune Toftgård§, Mario R. Capecchi¶¶, and Anders Jacobsson‡‖**

*From the ‡The Wenner-Gren Institute, The Arrhenius Laboratories F3, Stockholm University, SE-106 91 Stockholm, Sweden, the §Department of Bioscience and Center for Nutrition and Toxicology, Karolinska Institute, NOVUM, SE-141 57 Huddinge, Sweden, the ¶Department of Clinical Neuroscience, Sahlgren's University Hospital, SE-431 80 Mölndal, Sweden, the ‖Department of Medical Biochemistry and Biophysics, Karolinska Institute, SE-171 77 Stockholm, Sweden, the **Department of Dermatology Service, Veterans Affairs Medical Center, San Francisco, California, and the ¶¶Howard Hughes Medical Institute, University of Utah, Salt Lake City, Utah 84112*

Very little is known about the *in vivo* regulation of mammalian fatty acid chain elongation enzymes as well as the role of specific fatty acid chain length in cellular responses and developmental processes. Here, we report that the *Elovl3* gene product, which belongs to a highly conserved family of microsomal enzymes involved in the formation of very long chain fatty acids, revealed a distinct expression in the skin that was restricted to the sebaceous glands and the epithelial cells of the hair follicles. By disruption of the *Elovl3* gene by homologous recombination in mouse, we show that ELOVL3 participates in the formation of specific neutral lipids that are necessary for the function of the skin. The *Elovl3*-ablated mice displayed a sparse hair coat, the pilosebaceous system was hyperplastic, and the hair lipid content was disturbed with exceptionally high levels of eicosenoic acid (20:1). This was most prominent within the triglyceride fraction where fatty acids longer than 20 carbon atoms were almost undetectable. A functional consequence of this is that *Elovl3*-ablated mice exhibited a severe defect in water repulsion and increased trans-epidermal water loss.

Fatty acids consisting of up to 16 carbons are synthesized by the well studied fatty acid synthase complex (1). However, a significant amount of the fatty acids produced by fatty acid synthase are further elongated into very long chain fatty acids (VLCFA).[1]

VLCFA have been recognized as structural components in a variety of fat molecules such as glycerolipids and sphingolipids. They are found in virtually all cells and are major constituents of the brain, skin, and testis (2–4). Depending on their chain length and degree of unsaturation, they contribute to membrane fluidity and other chemical properties of the cell.

Formation of VLCFA is performed in the endoplasmic reticulum, in the early Golgi, and in mitochondria by membrane-bound enzymes, the former being more prominent (5, 6).

Recently, five mammalian genes, *Elovl1–5*,[2] whose protein products belong to a highly conserved family of microsomal enzymes involved in the formation of VLCFA, have been identified (7–10). All five genes show a diverse tissue-specific expression pattern indicating a unique role for different VLCFA in different cell types.

Although the general functions of the *Elovl* genes are partially understood (8–14), very little is known about the role of specific fatty acid chain length in cellular responses and developmental processes. The ELOVL3 protein has been suggested to be involved in the formation of saturated and monounsaturated fatty acyl chains containing up to 24 carbon atoms (9). *Elovl3* gene expression has only been detected in brown adipose tissue, liver, and skin (7, 9). To assess the *in vivo* role of ELOVL3, we disrupted the *Elovl3* gene by homologous recombination in mouse. Here we describe the characterization of *Elovl3* expression in skin and present evidence that ELOVL3 participates in the formation of certain VLCFA and triglycerides in certain cells of the hair follicles and the sebaceous glands and that these lipid compounds are essential for function of the skin.

MATERIALS AND METHODS

Elovl3 Gene Targeting Construct—A genomic liver DNA library from mouse strain 129/Sv cloned into the Lambda FIXII vector was used to isolate a DNA fragment containing the entire *Elovl3* gene (15). A 2.75-kb fragment between SacI and SalI upstream of the first exon was subcloned into the polylinker of the pBluescript SK plasmid in order to become the left arm (*LA*) in the *Elovl3* gene targeting construct (Fig. 1*A*). The SacI site was blunt ended by T4 DNA polymerase (New England Biolab) and turned into a NotI site by ligation of NotI primers (BioSource International). A 1.2-kb fragment containing a neomycin resistance gene (*neo*^{r}) was inserted into the compatible SalI site of the plasmid containing the 2.75-kb left arm fragment. The ligation between SalI and XhoI ends consequently destroyed the recognition site for respective digestion enzymes. A 5.30-kb SalI/SalI fragment downstream of the second exon of the *Elovl3* gene was ligated into the pBluescript SK plasmid and further digested with SalI and XhoI to receive a 2.77-kb fragment corresponding to the right arm (*RA*) in the *Elovl3* gene-targeting construct. This fragment was subcloned into the XhoI site of the vector containing the 2.75-kb left arm fragment and the *neo*^{r}

* This work was supported by grants from the Swedish Natural Science Research Council (to A. J.), from the Swedish Medical Research Council (to A. J. and J.-E. M.), from the Howard Hughes Medical Institute and the Mathers Charitable Foundation (to M. R. C.), and from the National Institutes of Health (WMH AR39448). The costs of publication of this article were defrayed in part by the payment of page charges. This article must therefore be hereby marked "*advertisement*" in accordance with 18 U.S.C. Section 1734 solely to indicate this fact.

‖ To whom correspondence should be addressed. Tel.: 46-8-164127; Fax: 46-8-156756; E-mail: anders.jacobsson@wgi.su.se.

[1] The abbreviations used are: VLCFA, very long chain fatty acids; TEWL, trans-epidermal water loss; ES, embryonic stem; HPTLC, high performance thin-layer chromatography.

[2] In accordance with the Mouse and Human Nomenclature Committees the assigning symbols for the mouse genes *Scc1*, *Ssc2*, and *Cig30* are changed to *Elovl1*, *Elovl2*, and *Elovl3*, respectively, and the human *HELO1* gene is changed to *ELOVL5*.

gene. The NotI/XhoI fragment from the resulting plasmid was ligated into a vector flanked by the thymidine kinase (*tk*) gene at the 3′-end.

Gene-targeting in ES Cells and Blastocyst Injection—The *Elovl3*-targeted construct was linearized by NotI and electroporated into the R1 embryonic stem (ES) cells derived from male 129/Sv agouti mice (16). ES cells were cultured as earlier described and subjected to positive/negative selection using G418 and FIAU as previously described (17, 18). ES cell DNA was prepared according to standard procedures (16). Probes as indicated in Fig. 1 and for the *neo*^{r} gene (not shown) were used to confirm ES cell clones heterozygous for the mutant *Elovl3* allele.

Elovl3-ablated ES cells were injected into C57BL/6J blastocysts and implanted into foster mothers (F1, CBAxC57BL6) according to standard procedures (19). The male offspring being the most chimeric, ~80% agouti and 20% black in the coat color, were bred with C57BL/6J females to generate offspring heterozygous for the mutation. Genomic DNA was prepared from mouse tails by the simplified mammalian DNA isolation as described earlier (20). Tail biopsies were collected from 3-week-old mice and used directly for DNA isolation.

The *Elovl3*-ablated mice were back-crossed with C57BL/6 (B&K Universal, Stockholm, Sweden) in the animal facility of the Institute. As control mice, we used heterozygote littermates or age-matched C57BL/6 mice that were bred under the same conditions as the *Elovl3*-ablated mice. Animals were fed *ad libitum* (rat and mouse standard diet No.1, BeeKay Feeds; B&K Universal, Stockholm, Sweden), had free access to water, and were kept on a 12:12-h light:dark cycle in single cages. Wild-type and *Elovl3*-ablated mice were bred in room temperature. Before exposing the animals to the cold, the mice were housed at 30 °C (thermoneutrality) for 10 days. Mice were placed in the cold (4 °C) for the times indicated.

Southern Blot Analysis of DNA from ES Cells and Mouse Tails—The DNA for the probes were purified according to the Jetsorb gel extraction kit (Genomed Inc.) and were labeled with [α-^{32}P]dCTP using a random primed labeling kit (Roche Applied Science). Ten μg digested DNA from mouse tails and ES cells was separated on 0.8% agarose gel and transferred to Hybond-N membrane (Amersham Biosciences) in 20× SSC. The membrane was prehybridized with a solution containing 5× SSC, 5× Denhardt's, 0.5% SDS, 50 mM sodium phosphate, 50% formamide, and 100 mg/ml degraded DNA from herring sperm (Sigma) at 45 °C. After prehybridization, the membrane was transferred to a similar solution containing the denatured probe. The hybridization was carried out overnight at 55 °C. Hybond-N membrane was washed twice in 2× SSC, 0.2% SDS at 30 °C for 20 min each and then once in 0.1× SSC, 0.2% SDS at 55 °C for 30 min. The filters were analyzed by phosphorimaging (Molecular Dynamics) and quantified with the ImageQuant program.

RNA Analysis—Total RNA was isolated using Ultraspec (Biotech Lab) from 50–100 mg (w/w) of each tissue as described earlier (7). For Northern blot analysis, 20 μg total RNA was separated on a 1.2% (w/v) formaldehyde agarose gel and blotted onto Hybond-N membrane (Amersham Biosciences) in 20× SSC. The hybridization procedure was identical to that for Southern blot analysis, except that hybridization was carried out overnight at 45 °C. The membrane was then washed twice in 2× SSC, 0.2% SDS at 30 °C for 20–30 min each and then twice in 0.1× SSC, 0.2% SDS at 50 °C for 45 min. A corresponding cDNA fragment of *Elovl3* (895-bp open reading frame) was used as a probe as previously described (7, 9). The filters were analyzed by phosphorimaging as for Southern analysis.

Histology—Skin biopsies of age- and sex-matched animals were taken from similar body sites. Skin samples were fixed overnight at 4 °C in a phosphate-buffered, pH 7.4, 4% formaldehyde solution. Semithin sections were stained with hematoxylin and eosin and examined by light microscopy.

For electron microscopy analysis, skin samples were taken at autopsy of 10-week-old mice and processed for electron microscopy. Samples were fixed overnight in Karnovsky's fixative, washed two times with 0.1 M cacodylate buffer, and post-fixed in either 1% osmium tetroxide (OsO_4) in 0.1 M cacodylate buffer, pH 7.3, or in ruthenium tetroxide (RuO_4) as described previously (21, 22). After fixation, samples were dehydrated in graded ethanol solutions and embedded in an Epon/epoxy mixture. Ultrathin sections were examined both with and without further contrasting with lead citrate in an electron microscope (Zeiss 1A; Carl Zewiss, Thornwood, NY) operated at 60 kV.

In Situ Hybridization—RNA probes were prepared from *Elovl3* open reading frame mouse cDNA. *In situ* hybridization was performed as described previously (23). Briefly, a 895-bp fragment corresponding to nucleotides 162–1056 in the *Elovl3* cDNA was cloned into a pCI-neo vector (Promega), appropriately linearized, and *in vitro* transcribed to obtain antisense and sense probes. Sections were treated with proteinase K (Sigma) and washed in 0.1 M triethanolamine buffer containing 0.25% acetic anhydride. Subsequently, sections were hybridized overnight with 2.5 × 10^6 cpm of labeled antisense or sense probe at 55 °C. Autography was carried out for 14 days. After development of the photographic emulsion, slides were stained with hematoxylin and eosin. The labeled sense strand served as negative control and did not show any labeling of cellular localization.

Epidermal Lipid Analysis—Hair was removed from the back of the mice, and skin was isolated by punching. After subcutaneous tissue was removed by scraping on ice, skin pieces were incubated in phosphate-buffered saline at 60 °C for 30 s, and epidermis was isolated by scraping on ice. Lipids were extracted using chloroform:methanol:water (2:4:1,6) overnight, and skin precipitates were stored for further extraction. Four ml chloroform:water (1:1) was added to the supernatant and incubated for 5 min at room temperature followed by centrifugation (2000 rpm). The water phase was discarded, and the organic phase was washed with chloroform:methanol:water (10:10:9). Non-extracted lipids from the original skin precipitates were sequentially extracted using chloroform:methanol (2:1, 1:1, 1:2). Extracts were pooled and evaporated under nitrogen.

TLC analysis was performed as described earlier (37). Total epidermal lipids were separated by HPTLC (Merck) with the following solvent sequence: 1) chloroform to 1.5 cm; 2) chloroform:methanol: acetone 76:16:8 (v/v) to 1 cm; 3) chloroform:methanol:hexyl acetate:acetone 86:4:1:10 (v/v) to 7 cm; 4) chloroform:methanol:acetone 76:20:4 (v/v) to 2 cm; 5) chloroform:methanol:diethyl ether:ethyl acetate:hexyl acetate:acetone 72:4:4:1:4:16 (v/v) to 7,5 cm; 6) *n*-hexane: diethyl ether:ethyl acetate 80:16:4 (v/v), and 7) *n*-hexane:diethyl ether:acetic acid 65:35:1 (v/v) to the top of the plate. Lipids were visualized after treatment with cupric acetate-phosphoric acid and heating to 160 °C for 15 min.

Hair Lipid Analysis—Hair from adult mice was extracted and filtered twice with 20 ml acetone for 15 min. The two extracts were combined and allowed to evaporate to dryness in glass vials. The amount of dry lipids was calculated by subtracting the weight of empty vials. Equal amounts of lipids (120 μg) were dissolved in acetone and applied to each lane on a Whatman HPTLC silica G plate and separated according to Downing (24). Briefly, the plate was previously run with chloroform, placed in an oven at 105 °C for 30 min, and then immediately cooled down to room temperature. The samples were spotted onto the plate and resolved in hexane. The plates were removed and air dried for 15 min. The plates were then run in toluene until the solvent front reached the end of the plate. After the plates were air dried for 15 min, a third phase containing hexane:ether:acetic acid (70:30:1) was run. The TLC plates were stained with sulfuric acid:ethanol (1:1) and charred at 150 °C. Lipids were analyzed by scanning densitometry of digital pictures taken from the TLC plate by phosphorimaging (Molecular Dynamics) with the ImageQuant program.

Mass Spectrometry Analysis—For the fatty acid determinations, 2 ml chloroform:methanol:water (60:30:4.5) extract of hair lipids was evaporated and dissolved in 2 ml 2.5% sulfuric acid in methanol. Acidic methanolysis was performed at 80 °C for 16 h. Formed fatty acid methyl esters were purified by preparative TLC in dichloromethane. Mass spectrometry analysis was performed on Fison MD 800 equipment with on-column injection. A DB 1 (J&W) capillary column 30 m × 0.32 mm was used for the separation.

Water Retention Assay and Temperature Measurement—Weight or colonic temperature was measured (RET-3 rectal thermometer; Physitemp Instruments Inc.) once for each adult mouse prior to swimming. Mice were allowed to swim in water at 30 °C for 2 min. Excessive water was eliminated by allowing the mice to walk on paper towels for a few seconds. Weight or colonic temperature was recorded every 5 min at 22 °C. Between each measurement the mice were kept individually in empty plastic cages. The hair water content was calculated by subtracting the preswim weight from the postswim weight.

Trans-epidermal Water Loss (TEWL) Analysis—Mice were anesthetized with 2.5% avertin by intraperitoneal injection at a concentration of 0.014 ml/g body weight. The evaporimeter (EP 1C; Servomed, Göteborg, Sweden) was run for at least 15 min prior to use. The evaporimeter was placed on 1 cm^2 of shaved skin on the back of the animal in an open chamber. During the measurement, the evaporimeter was allowed to stabilize for 30 s before the value was recorded. All measurements were performed according to the guidelines from the standardization group of contact dermatitis (25).

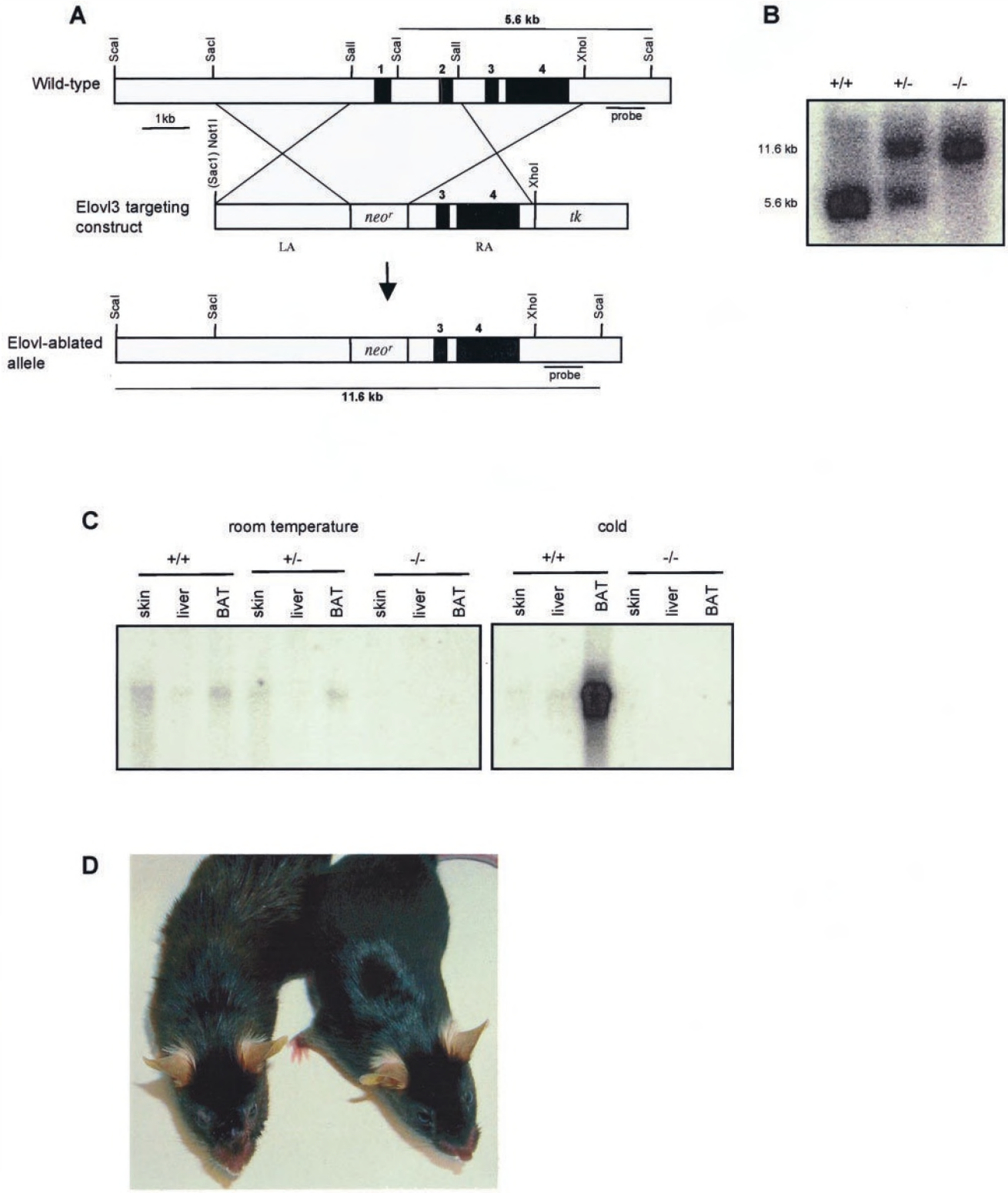

FIG. 1. **Generation of *Elovl3*-ablated mice.** *A*, schematic drawing of the *Elovl3* gene-targeting construct. The targeting construct for *Elovl3* replaces the transcription start and exons 1 and 2 of the genomic DNA. Location of the probe for Southern analysis is indicated by *bars* underneath the wild-type and mutated allele. The mutated *Elovl3* allele differs from the wild-type allele in the absence of an internal ScaI site due to homologous recombination. The *lines* indicate the distances between ScaI sites. *Black boxes* represent exons and are denoted with *numbers* above them. The thymidine kinase selection gene is denoted by *tk*. *B*, genomic DNA from different genotypes of F1 offspring were digested with ScaI and analyzed with Southern blot to distinguish between mice being wild-type (+/+), heterozygous (±), or homozygous (−/−) for the mutant *Elovl3* allele. Digestion yielded the 11.6- and 5.6-kb fragments, respectively, detected by the probe. *C*, Northern analysis of *Elovl3* expression in brown adipose tissue (*BAT*), liver, and skin. Tissues were taken from mice kept at room temperature (22 °C) or exposed to cold (4 °C) for 15 days. 10 μg total RNA was loaded in each lane. After electrophoresis and transfer, the membranes were probed with a 900-bp *Elovl3* open reading frame fragment. *D*, phenotype of *Elovl3*-ablated mice. Heterozygote (*right*) and homozygote (*left*) *Elovl3*-ablated mice at 9 weeks.

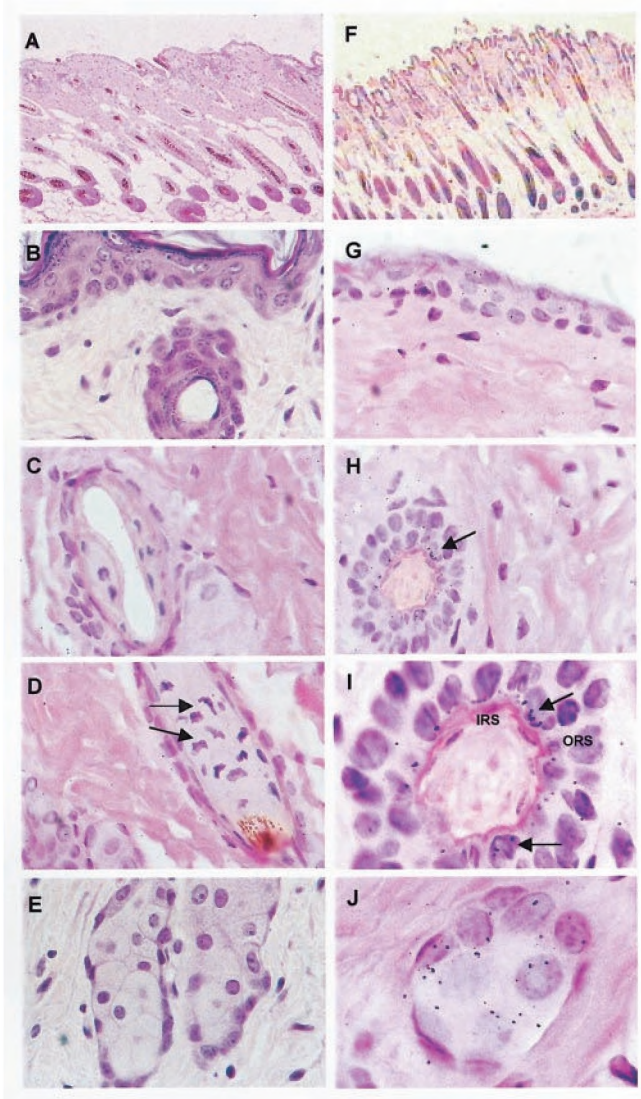

FIG. 2. **Histological analysis of the skin from *Elovl3*-ablated mice and cell-specific expression of *Elovl3* mRNA in hair follicles and sebaceous glands in wild-type skin.** Microscopic overview of the skin from the back of an *Elovl3*-ablated mouse (*A–E*) and wild-type mouse (*F–J*) at the age of 9 weeks showing epidermis, hair follicles, and dermis. *A*, in the *Elovl3*-ablated mouse, the normal hair is missing in the upper part of several hair follicles though the hair seems normal in the lower parts. *B*, in higher magnification, an increased thickness of the epidermis and hypergranulation is seen both in epidermis and in the hair follicle. *C*, transverse section of a hair follicle shows abnormal epithelial cells. *D*, the inner cell layer of the outer root sheath appears abnormal with irregularly shaped nuclei (*arrows*). *E*, hyperplastic and enlarged sebocytes are seen in the sebaceous glands. *G*, by *in situ* hybridization very low *Elovl3* expression is seen in a cross-section of epidermis of wild-type skin. *H*, horizontal section showing specific expression of *Elovl3* in the epithelial cells of a hair follicle (*arrow*, *black grains*). *I*, a higher magnification of the epithelial cells of the hair follicle showing abundant *Elovl3* mRNA signal in the cells of the inner layer of the outer root sheath (*ORS*) of the hair follicle (*arrows*). *IRS*, inner root sheath. *J*, a strong *Elovl3* mRNA signal (*black grains*) was detected in normal sebocytes. *A–E*, no *Elovl3* mRNA signal was detected in *Elovl3*-ablated mice. (All sections are counterstained with hematoxylin and eosin).

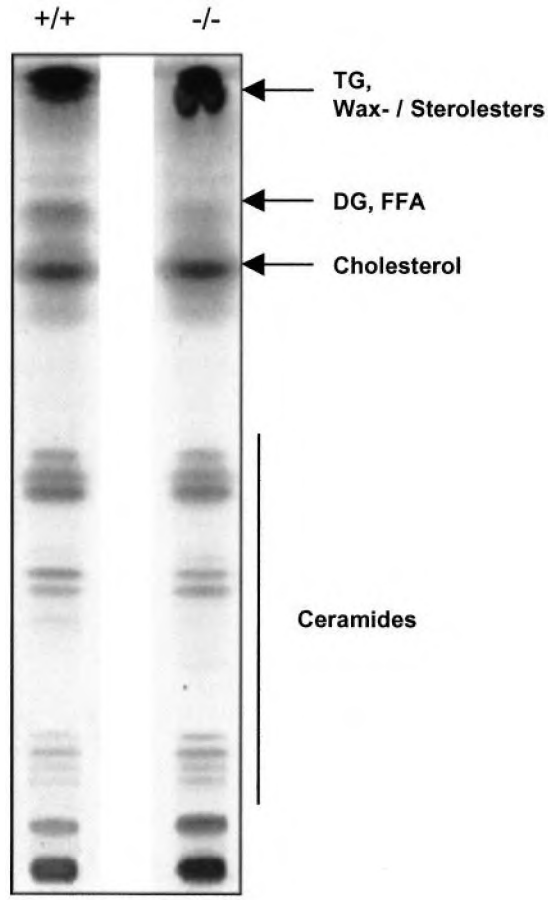

FIG. 3. **Abnormal content of neutral skin lipids of *Elovl3*-ablated mice.** Equal amounts of epidermal lipids (120 μg) from wild-type (+/+) and *Elovl3*-ablated (−/−) mice were separated by HPTLC. The *arrows* and *vertical line* indicate the transfer area of triglycerides and sterol and wax esters, diacylglycerols and free fatty acids, cholesterol, and ceramides, respectively, according to lipid standards.

RESULTS

Generation of Elovl3-ablated Mice—A SalI fragment, including the transcription start site, exon 1 and 2 of the *Elovl3* gene, was deleted by homologous recombination in R1 ES cells due to insertion of a *neo*^{r} gene (Fig. 1*A*). Targeted ES cells were microinjected into blastocysts of C57BL/6J (B6) mice. Two independent chimeric lines were found to transmit the *Elovl3* disruption through the germline, which was confirmed by Southern blot analysis (Fig. 1*B*). The 5.6-kb ScaI genomic fragment representing the wild-type *Elovl3* allele is absent in *Elovl3*-ablated mice and replaced by a 11.6-kb fragment that hybridizes to the probe (Fig. 1, *A* and *B*).

To determine the *Elovl3* expression, Northern blot analyses were performed with total RNA isolated from brown adipose tissue, skin, and liver, *i.e.* organs that have been shown to express *Elovl3* (7), from wild-type and *Elovl3*-ablated mice (Fig. 1*C*). The gene disruption was particularly clear upon cold stimulation, where no *Elovl3* mRNA was detected in brown adipose tissue from *Elovl3*-ablated mice, a site with the highest reported *Elovl3* expression (7).

Phenotype Characteristics—Interestingly, the *Elovl3*-ablated mice did not show any indications of impaired liver or brown adipose tissue function. The striking feature that distinguished *Elovl3*-ablated mice from wild-type or heterozygous littermates was a tousled and reduced fur content over the whole body (Fig. 1*D*) that was noticeable within 2 weeks of age when the hair was formed and sustained throughout the life span. In addition, mice older than approximately six months showed irritated skin and distinctive scratch marks on the chin that resembled eczematous skin. The mice grew normally and were fertile. Offspring genotypes obtained from heterozygous F1 intercrosses showed normal Mendelian distribution.

Microscopic Distinctions of the Skin in Elovl3-ablated Mice—Grossly, the epidermis of the *Elovl3*-ablated mice appeared normal, but parts of the epidermis were thicker with observed hy-

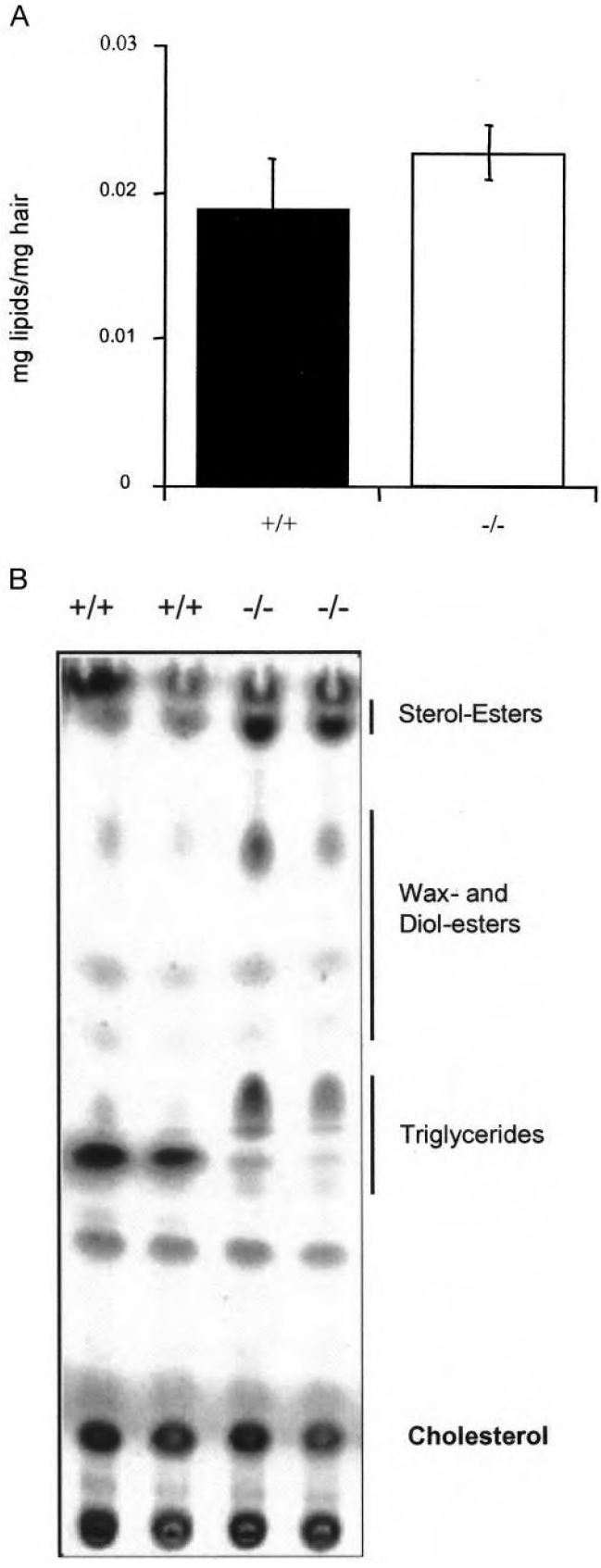

FIG. 4. **Abnormal content of hair lipids of *Elovl3*-ablated mice.** *A*, normal and mutated mice had similar total hair lipid production. Lipid content in the hair was determined in 10 wild-type (+/+) and 8 *Elovl3*-ablated (−/−) mice, respectively, with values expressed as mean ± S.E. *B*, equal amounts of hair lipids (120 μg) loaded on silica gel 60 TLC plate (20 × 20 cm). The *vertical lines* indicate the transfer area of sterol esters, wax and diol esters and triglycerides according to lipid standards.

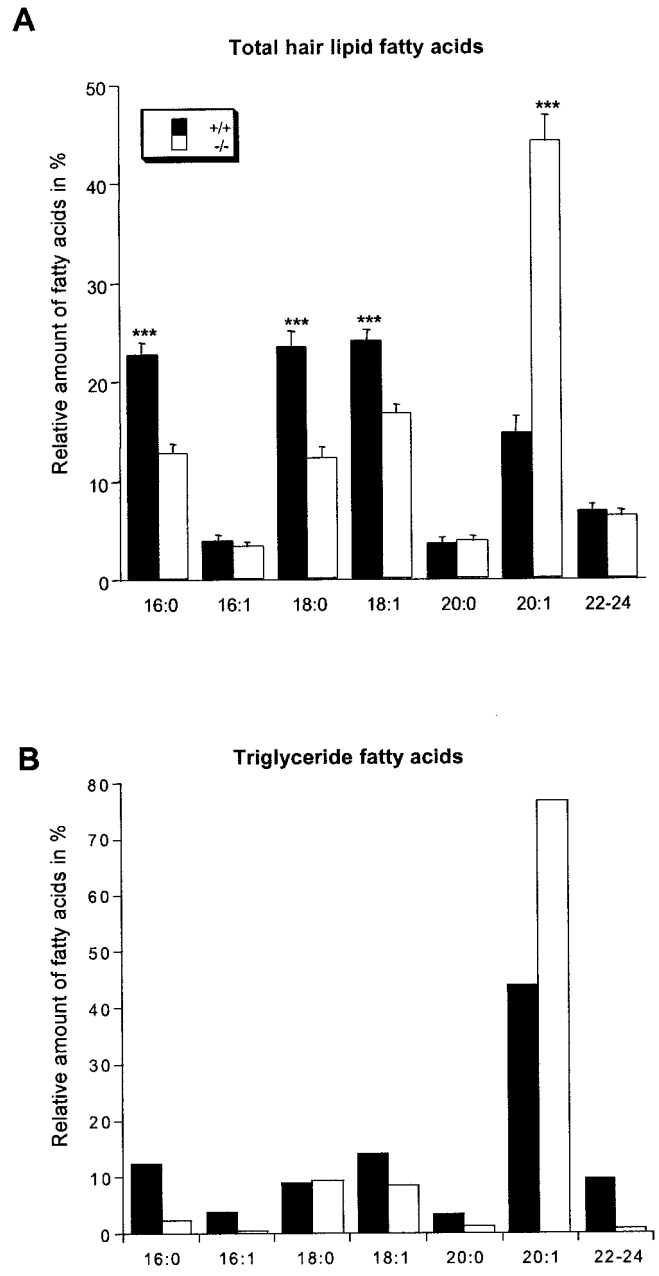

FIG. 5. **Mass spectroscopic analysis of hair lipids.** *A*, gas chromatography-mass spectrometry analysis of the acyl chain content in acetone-extracted lipids from the hair of wild-type (*black bars*) and *Elovl3*-ablated mice (*open bars*). The *22–24 bars* indicate both saturated and monounsaturated fatty acids. Each *bar* represents the mean value ± S.E. of 10 animals. p = * < 0.05, ** < 0.01, *** < 0.001. *B*, detailed gas chromatography-mass spectrometry analysis of the acyl chain content within the triglyceride fraction of hair lipids from the hair of wild-type (+/+) and *Elovl3*-ablated mice (−/−). Each *bar* represents the relative mean value of two triglyceride fractions pooled from two mice of each strain.

pergranulation (Fig. 2, *A* and *B*). The nuclei of the hair follicle cells seemed irregularly shaped, especially within the cells in the inner layer of the outer root sheath (Fig. 2, *C* and *D*), and as in the epidermis scattered hypergranulation was seen (Fig. 2, *A* and *C*). In many of the hair follicles, normal hair was missing in the upper part, though the hair seemed normal in the lower parts of the follicles. However, the most evident finding was a general hyperplasia of the sebaceous glands (Fig. 2*E*).

Cell-specific Expression of Elovl3 in the Skin—Under normal conditions, *Elovl3* is sparsely expressed in the skin. To delineate this expression, we performed *in situ* hybridization anal-

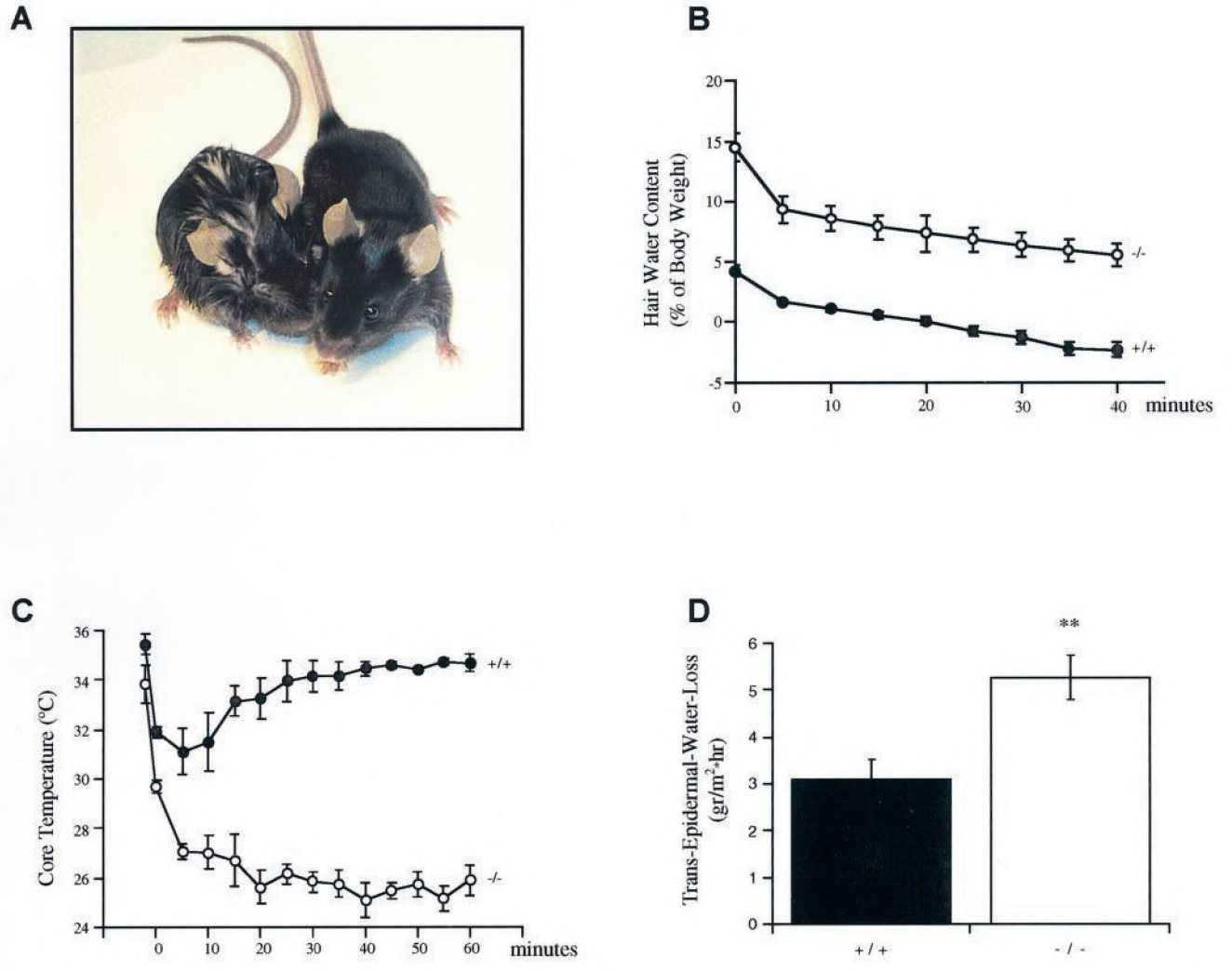

FIG. 6. **Defects in water barrier of *Elovl3*-ablated mice.** *A*, 20 min after a 2-min swim in 30 °C, *Elovl3*-ablated mice (*left*) are still wet compared with wild-type mice (*right*). *B*, impaired water repulsion in *Elovl3*-ablated mice. *Elovl3*-ablated mice absorb more water during the swim than wild-type mice. *Error bars* indicate mean ± S.E. of seven wild-type and *Elovl3*-ablated mice,respectively. *C*, increased water absorption induces hypothermia in *Elovl3*-ablated mice compared with wild-type mice. After exposure to water, rectal temperature was measured every 5 min for one hour. Each point is mean ± S.E. in four experiments. *D*, impaired skin barrier in *Elovl3*-ablated mice because of trans-epidermal water loss in healthy wild-type mice (+/+) and *Elovl3*-ablated mice (−/−). The values are expressed as mean ± S.E. of 10 mice in each group. $p = <0.01$ in comparison with healthy animals.

ysis. In the wild-type mice, a strong *Elovl3* mRNA signal was seen in the cells of the inner layer of the outer root sheath (Fig. 2, *H* and *I*) of the hair follicles and in the sebocytes of the sebaceous glands (Fig. 2*J*). In epidermis the *Elovl3* mRNA signal was very low (Fig. 2*G*), and in fibroblasts no detectable signal was seen. In the *Elovl3*-ablated mouse, there was no detectable *Elovl3* mRNA signal in any cell type (Fig. 2, *A–E*). No signal was detected in tissues hybridized with the sense probe (data not shown).

Disturbed Epidermal Skin Lipid Content of Elovl3-ablated Mice—Regarding the restricted *Elovl3* expression in the skin and the abnormal morphology of the hair follicles and pilosebaceous system in the *Elovl3*-ablated mice, we suspected the lipid composition of the secreted sebum to be affected. Because the sebaceous glands are appendages of the epidermis connected to hair follicles and secrete the sebum onto the skin surface, we analyzed the lipid content of the epidermis, including the outermost part, stratum corneum, by thin layer chromatography. From this it was clear that the major difference between wild-type and *Elovl3*-ablated mice was observed in the most mobile fractions, which were a mixture of neutral lipids, such as triglycerides and wax and sterol esters, which are normal constituents of the sebum (Fig. 3). In contrast, there was no major difference between the more polar fractions where the different sphingolipid-based ceramide moieties migrate. A similar pattern was also seen when total skin was analyzed (not shown), suggesting a selective unbalance in the neutral lipids of the epidermis and hair.

Disturbed Lipid Content in the Hair of Elovl3-ablated Mice—Although there was a general tendency toward more acetone-extractable lipids in the hair of *Elovl*-ablated mice, the total amount of hair lipids did not significantly differ from the wild-type mice (Fig. 4*A*). When we analyzed the hair lipids by TLC, the fractions containing triglycerides, wax esters, diol esters, and sterol esters formed a different TLC pattern between the two strains of mice (Fig. 4*B*). The most obvious difference was a shift in the amount of specific lipid components in the area where the triglycerides were localized (Fig. 4*B*). Densitometric analysis displayed a 10-fold decrease in a relatively more hydrophilic component, which was counteracted by a 10-fold increase in a relatively more hydrophobic component.

Mass Spectrometric Analysis of Hair Lipids—The ELOVL3

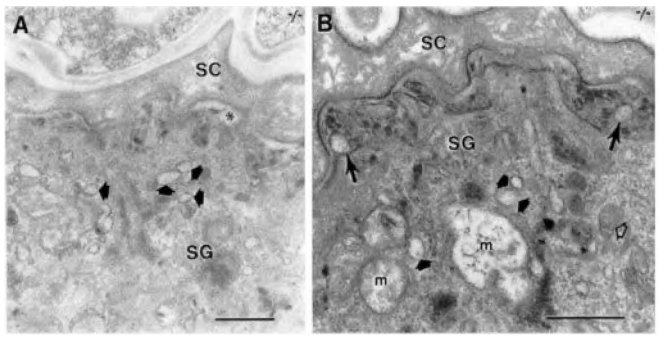

FIG. 7. **Mutant epidermis (−/−) displays abnormal lamellar body contents.** *A* and *B*, *small solid arrows* indicate abnormal lamellar body contents in stratum granulosum (*SG*). *B*, normal internal contents are rarely seen (*small open arrow*). *A*, secreted lamellar body contents at stratum granulosum (*SG*)-stratum corneum (*SC*) interface are loosely organized (*asterisk*), and contain electron lucent droplets (*B*, *larger arrow*). *m* indicates mitochondria. Samples were in osmium tetroxide post-fixative; *magnification bars* = 0.5 μm.

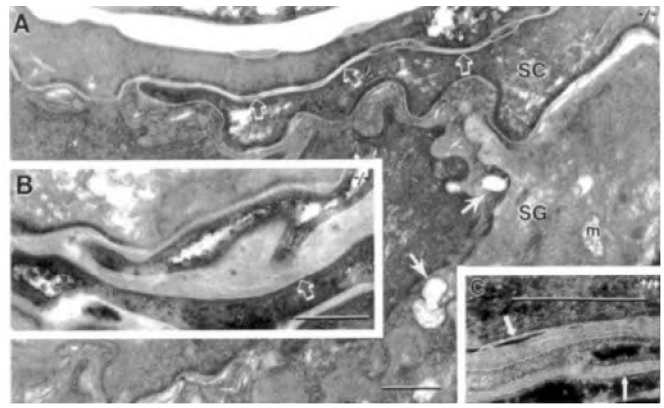

FIG. 8. **Extracellular domains are abnormal in *Elovl3*-ablated (−/−) stratum corneum (*SC*).** *A*, note again electron-lucent droplets at stratum granulosum (*SG*)-stratum corneum (*SC*) interface (*solid arrows*). Extracellular domains above SG-SC interface display a paucity of lamellar bilayers (*A*, *open arrows*) and abundant amorphous, non-lamellar material (*B*). *C*, normal-appearing extracellular bilayers (*arrows*) in wild-type (+/+) SC. *m* indicates mitochondria. Samples were in uthenium tetroxide post-fixative; *magnification bars* = 0.25 μm.

protein has been suggested to be involved in the formation of fatty acyl chains containing up to 24 carbon atoms (9). When we compared the acyl chain content in acetone-extracted lipids from the hair of wild-type and *Elovl3*-ablated mice by mass spectrometry analysis, there was a remarkable increase in eicosenoic acid (20:1 (n-9)) in the *Elovl3*-ablated mice. The amount increased from 14 to 43% of total lipids (Fig. 5*A*). In contrast, there was about a 40% decrease in C16:0, C18:0 and C18:1 (n-9) fatty acids, which suggests that the regulation of saturated and monounsaturated (n-9) fatty acid levels, in general, is affected in *Elovl3*-ablated mice. Surprisingly, we did not detect a decrease in VLCFA longer than 20 carbon atoms in the *Elovl3*-ablated mice.

Because in the TLC experiment we had observed a dramatic mobility shift within the area where the triglycerides migrated, we analyzed the fatty acid profile within this fraction of the hair lipids. Similar to what was detected in the total hair lipids, there was an enormous amount of 20:1 (n-9) in the *Elovl3*-ablated mice (77%) compared with wild-type mice (44%), which was associated with a reduced amount of shorter saturated and monounsaturated fatty acids (Fig. 5*B*). However, in contrast to the data on total lipids, the amount of saturated and monounsaturated fatty acids containing 22–24 carbon atoms within the triglyceride fraction was almost undetectable (less than 1%) in the *Elovl3*-ablated mice compared with 10% in the wild-type animals. The sterol and wax ester fraction showed a similar profile difference for the fatty acids up to 20:1 between the wild-type and *Elovl3*-ablated mice. However, in contrast to the triglyceride fraction, there was no decrease in 22–24 fatty acids within this fraction. This implies a specific role of *Elovl3* in regulating the fatty acid composition within the triglycerides, which if disrupted have effects on the neutral lipids of the sebum in general.

Defective Water Repulsion and Thermoregulation in Elovl3-ablated Mice—To investigate the relevance of *Elovl3* for normal function of the hair, we performed a water repulsion experiment in which the animals were allowed to swim at 30 °C for 2 min. From this, it became evident that *Elovl3*-ablated mice showed an impaired ability to repel water because they absorbed three times as much water as wild-type mice (Fig. 6, *A* and *B*), about 14% of their body mass compared with 4% for the wild-type mice. However, the rate of water evaporation from the skin during the following 40 minutes of the test proved to be equal for the *Elovl3*-ablated and wild-type mice (Fig. 6*B*).

Surprisingly, even though the *Elovl3* mRNA level has been shown to be increased about 100-fold in the brown adipose tissue of cold-exposed wild-type mice (7), the *Elovl3*-ablated mice did not show impaired brown fat activity (*i.e.* loss of body temperature) when exposed to the cold for even as long as several months.[3] To see whether impaired water repulsion of the *Elovl3*-ablated mice also leads to impaired thermoregulation, body temperature was measured in wild-type and *Elovl3*-ablated mice after a 2-min swim in 30 °C. The *Elovl3*-ablated and wild-type animals had the same body temperature at ambient temperature (22 °C) before the swim (Fig. 6*C*). After the swim, wild-type mice experienced a drop in core temperature to a lowest value of 31 °C after 5 min. The core body temperature returned to baseline level after approximately 20 min, which also coincided with the return of a completely dry fur (Fig. 6, *B* and *C*). In contrast, the core temperature of *Elovl3*-ablated mice decreased to 26 °C and remained at that temperature for at least one hour, which also correlated with wet fur (Fig. 6, *B* and *C*). So, even if the *Elovl3*-ablated mice can withstand a 4 °C cold exposure, they are unable to maintain their body temperature with wet fur even at room temperature.

Increased Trans-epidermal Water Loss in Elovl3-ablated Mice—Because a major function of the skin is to provide a barrier to water transmission, we hypothesized that the *Elovl3*-ablated mice may have a disturbed water barrier resulting in an increased TEWL. To test this, we quantified the diffusion of water through the skin by a TEWL test. As shown in Fig. 6*D*, the *Elovl3*-ablated mice had a 70% higher rate of evaporation compared with wild-type mice, indicating a higher water loss due to skin barrier impairment.

Abnormal Lamellar Body Content in Epidermis of Elovl3-ablated Mice—To delineate the basis for the cutaneous abnormalities induced by the deficiency of *Elovl3*, electron micrographs from mutant and wild-type epidermis were compared. *Elovl3*-deficient epidermis displayed lamellar bodies with abnormal contents (Figs. 7 and 8, *solid arrows*), as well as poorly organized extracellular membrane domains (Figs. 7, *A* and *B*, and 8, *A* and *B*), compared with the highly ordered membrane lipid domains in normal (+/+) epidermis (Fig. 8*C*). Intra- and extracellular domains contained electron-lucent domains consistent with abnormal neutral lipid accumulation (Figs. 7 and 8). Extracellular domains above stratum granulosum (*SG*)-stratum corneum (*SC*) interface display a paucity of lamellar bilayers (Fig. 8, *A* and *B*, *open arrows*) and abundant amorphous, non-lamellar material (Fig. 8*B*). These studies indicate

[3] A. Jacobsson, unpublished data.

that the deficiency of *Elovl3* disrupts normal lamellar body formation and subsequent generation of extracellular lamellar membranes necessary for normal epidermal permeability barrier function. The presence of both intra- and extracellular lipid droplets is consistent with inappropriate accumulation of non-barrier, neutral lipids in the epidermis of *Elovl3*-ablated animals. Thus, the abnormal barrier function, *i.e.* elevated TEWL, reflects altered lipid production and/or accumulation within the epidermis that results in abnormal membrane domains in the stratum corneum.

DISCUSSION

We report here a novel mechanism involving the *Elovl3* gene product in the protective function of the skin. From TLC experiments, it became evident that the *Elovl3*-ablated mice had modified levels of specific ester components in their hair lipids. The fact that the sebaceous glands were hyperplastic implied the existence of a compensatory mechanism. The fatty acid analysis suggested that this was because of an accumulation of sebum lipids by reason of a deficiency in further elongation of 20:1 for production particularly of triglycerides.

The marked increase in TEWL of the *Elovl3*-ablated mice indicates that the stratum corneum in affected animals does not provide for normal barrier function. Ultrastructural analysis, using electron microscopy, revealed that stratum corneum extracellular membrane domains contained areas with a significant amount of neutral lipid accumulation. In addition, both normal- and abnormal-appearing lamellar bodies and extracellular membrane domains were evident in *Elovl3*-deficient epidermis. These findings reveal that the barrier abnormality induced by *Elovl3* deficiency is a consequence of membrane abnormalities within the stratum corneum, likely because of abnormal lipid ratios within these critical membrane domains. This agrees with our inability to detect any major differences within the sphingolipid fraction of the epidermis between *Elovl3*-ablated and wild-type mice but rather within the more hydrophobic lipid fractions. Because the expression of *Elovl3* is restricted to certain cells within the hair follicles and the sebaceous glands, the deficiency in barrier integrity of the stratum corneum is probably because of an imbalance in the lipid content of the sebum.

In addition to the imbalance in the lipid content of the sebum, the hair phenotype could be explained by the absence of *Elovl3* expression in the inner cell layer of the outer root sheath; our hypothesis is that these cells have lost their normal function. Although an exact function of these cells is still unknown, our data suggest a role of *Elovl3* in the synthesis of specific saturated and/or monounsaturated VLCFA, essential for normal function of the hair. In addition, even though the hair of the *Elovl3*-ablated mice contained as much lipids as the wild-type mice, the mechanism behind the impaired synthesis of *Elovl3*-based VLCFA and the inability of the hair to repel water is still unknown.

Interestingly, apart from the *Elovl3* mutation, there are three additional gene mutations, *asebia*, *scraggly*, and diacylglycerol acyltransferase 1 (*Dgat1*)-ablated mice (26–28) that give rise to very similar phenotypic effects: hair loss, skin defects, and abnormalities in sebaceous lipid composition. The *asebia* mutation suffers from inability to synthesize specific monounsaturated fatty acids, preferentially palmitoleoyl- and oleoyl-CoA (16:1 and 18:1, respectively), because of a mutation in the steroyl-CoA desaturase 1 and 3 (SCD1 and SCD3) gene (29–31). However, in contrast to the hyperplasia seen in the sebaceous glands of *Elovl3*-ablated mice, *asebia* develop hair loss and abnormal hair follicles because of sebaceous gland hypoplasia (29, 32–35). The gene product of *scraggly* is not yet identified. In these mutants, the loss of hair phenotype is not an immediate event but develops with increased age. Despite a higher amount of total hair lipids from *scraggly* than in wild-type mice, the sebaceous glands appeared to be normal in structure. In the *Dgat1*-ablated mice, when the final step of triglyceride synthesis was eliminated, an impaired and reduced production of neutral lipids in the sebum was detected (28).

Recently, Fluhr *et al.* (36) demonstrated that in the *asebia* mouse the sebaceous gland-derived glycerol, a major contributor of stratum corneum hydration, is impaired, which emphasizes the importance of glycerol generation from triglyceride in the sebaceous glands. This may be of great importance regarding the phenotype of *scraggly*, *Dgat1*-, and *Elovl3*-ablated mice as well, which all have a disturbed triglyceride synthesis within their hair lipids.

Although the abnormal fatty acid composition in the hair lipids of *asebia*, *scraggly*, *Dgat1*-, and *Elovl3*-ablated mice results in an abnormal synthetic or degenerative process that is necessary for completion of normal hair and sebum production, there are clear histopathological differences in the hair follicles and in the sebaceous glands between these mutants. In strong contrast to the *asebia* and the *Dgat1*-ablated mice, which phenotype is associated with dry fur and atrophic sebaceous glands, *Elovl3*-ablated mice showed both hyperthrophic sebaceous glands and an overproduction of certain lipids. This suggests that *Elovl3*-based VLCFA are essential for maintaining a balanced lipid metabolism in the sebaceous glands.

In summary, our data show that the length of the carbon chain of VLCFA in the skin is of high significance, not only as structural components but also as non-membrane-bound lipid components such as triglycerides and sterol esters. We also show that this is under strict regulatory control in certain cells, which in case of irregularity can have detrimental effects on lipid metabolism and, consequently, on the development and maintenance of hair and skin function.

Acknowledgments—We thank B. Leksell, S. Sundberg, and B. Jungbjer for technical assistance and B. Forslind and P. Fredman for valuable discussions.

REFERENCES

1. Smith, S. (1994) *FASEB J.* **8,** 1248–1259
2. Stewart, M. E., and Downing, D. T. (1991) *Adv. Lipid Res.* **24,** 263–301
3. Coniglio, J. G. (1994) *Prog. Lipid Res.* **4,** 387–401
4. Poulos, A. (1995) *Lipids* **30,** 1–14
5. Cinti, D. L., Cook, L., Nagi, M. N., and Suneja, S. K. (1992) *Prog. Lipid Res.* **31,** 1–51
6. David, D., Sundarababu, S., and Gerst, J. E. (1998) *J. Cell Biol.* **143,** 1167–1182
7. Tvrdik, P., Asadi, A., Kozak, L. P., Nedergaard, J., Cannon, B., and Jacobsson, A. (1997) *J. Biol. Chem.* **272,** 31738–31746
8. Leonard, A. E., Bobik, E. G., Dorado, J., Kroeger, P. E., Chuang, L.-T., Thurmond, J. M., Parker-Barnes, J. M., Das, T., Huang, Y.-S., and Mukerji, P. (2000) *Biochem. J.* **350,** 765–770
9. Tvrdik, P., Westerberg, R., Silve, S., Asadi, A., Jakobsson, A., Cannon, B., Loison, G., and Jacobsson, A. (2000) *J. Cell Biol.* **149,** 707–717
10. Zhang, K., Kniazeva, M., Han, M., Li, W., Yu, Z., Yang, Z., Li, Y., Metzker, M. L., Allikmets, R., Zack, D. J., Kakuk, L. E., Lagali, P. S., Wong, P. W., MacDonald, I. M., Sieving, P. A., Figueroa, D. J., Austin, C. P., Gould, R. J., Ayyagari, R., and Petrukhin, K. (2001) *Nat. Genet.* **27,** 89–93
11. Oh, C. S., Toke, D. A., Mandala, S., and Martin, C. E. (1997) *J. Biol. Chem.* **272,** 17376–17384
12. Moon, Y. A., Shah, N. A., Mohapatra, S., Warrington, J. A., and Horton, J. D. (2001) *J. Biol. Chem.* **276,** 45358–45366
13. Matsuzaka, T., Shimano, H., Yahagi, N., Yoshikawa, T., Amemiya-Kudo, M., Hasty, A. H., Okazaki, H., Tamura, Y., Iizuka, Y., Ohashi, K., Osuga, J., Takahashi, A., Yato, S., Sone, H., Ishibashi, S., and Yamada, N. (2002) *J. Lipid Res.* **43,** 911–920
14. Moon, Y. A., and Horton, J. D. (2003) *J. Biol. Chem.* **278,** 7335–7343
15. Tvrdik, P., Asadi, A., Kozak, L. P., Nuglozeh, E., Parente, F., Nedergaard, J., and Jacobsson, A. (1999) *J. Biol. Chem.* **274,** 26387–26392
16. Nagy, A., Rossant, J., Nagy, R., Abramow-Newerly, W., and Roder, J. C. (1993) *Proc. Natl. Acad. Sci. U. S. A.* **90,** 8424–8428
17. Thomas, K. R., and Capecchi, M. R. (1987) *Cell* **51,** 503–512
18. Mansour, S. L., Thomas, K. R., and Capecchi, M. R. (1988) *Nature* **336,** 348–352
19. Gossler, A., Doetschman, T., Korn, R., Serfling, E., and Kemler, R. (1986) *Proc. Natl. Acad. Sci. U. S. A.* **83,** 9065–9069
20. Laird, P. W., Zijderveld, A., Linders, K., Rudnicki, M. A., Jaenisch, R., and Berns, A. (1991) *Nucleic Acids Res.* **19,** 4293–4293

21. Madison, K. C., Swartzendruber, D. C., Wertz, P. W., and Downing, D. T. (1987) *J. Investig. Dermatol.* **88,** 714–718
22. Hou, S. Y., Mitra, A. K., White, S. H., Menon, G. K., Ghadially, R., and Elias, P. M. (1991) *J. Investig. Dermatol.* **96,** 215–223
23. Nilsson, M., Unden, A. B., Krause, D., Malmqwist, U., Raza, K., Zaphiropoulos, P. G., and Toftgård, R. (2000) *Proc. Natl. Acad. Sci. U. S. A.* **97,** 3438–3443
24. Downing, D. T. (1968) *J. Chromatogr.* **38,** 91–99
25. Pinnagoda, J., Tupker, R. A., Agner, T., and Serup, J. (1990) *Contact Dermatitis* **22,** 164–178
26. Josefowicz, W. J., and Hardy, M. H. (1978) *Genet. Res.* **31,** 53–65
27. Herron, B. J., Bryda, E. C., Heverly, S. A., Collins, D. N., and Flaherty, L. (1999) *Mamm. Genome* **10,** 864–869
28. Chen, H. C., Smith, S. J., Tow, B., Elias, P. M., and Farese, R. V., Jr. (2002) *J. Clin. Investig.* **109,** 175–181
29. Zheng, Y., Eilertsen, K. J., Ge, L., Zhang, L., Sundberg, J. P., Prouty, S. M., Stenn, K. S., and Parimoo, S. (1999) *Nat. Genet.* **23,** 268–270
30. Zheng, Y., Eilertsen, K. J., Ge, L., Zhang, L., Sundberg, J. P., Prouty, S. M., Stenn, K. S., and Parimoo, S. (1999) *Nat. Genet.* **23,** 268–270
31. Miyazaki, M., Kim, Y. C., Gray-Keller, M. P., Attie, A. D., and Ntambi, J. M. (2000) *J. Biol. Chem.* **275,** 30132–30138
32. Gates, A. H., and Karasek, M. (1965) *Science* **148,** 1471–1473
33. Brown, W. R., and Hardy, M. H. (1989) *J. Investig. Dermatol.* **92,** 126–129
34. Williams, D., and Stenn, K. S. (1994) *Dev. Biol.* **165,** 469–479
35. Sundberg, J. P., Boggess, D., Sundberg, B. A., Eilertsen, K., Parimoo, S., Filippi, M., and Stenn, K. (2000) *Am. J. Pathol.* **156,** 2067–2075
36. Fluhr, J. W., Mao-Qiang, M., Brown, B. E., Wertz, P. W., Crumrine, D., Sundberg, J. P., Feingold, K. R., and Elias, P. M. (2003) *J. Investig. Dermatol.* **120,** 728–737
37. Uchida, Y., Hara, M., Nishio, H., Sidransky, E., Inoue, S., Otsuka, F., Suzuki, A., Elias, P. M., Holleran, W. M., and Hamanaka, S. (2000) *J. Lipid Res.* **41,** 2071–2082